

## Four-Dimensional Quantum Hall Effect with Ultracold Atoms

H. M. Price,<sup>1</sup> O. Zilberberg,<sup>2</sup> T. Ozawa,<sup>1</sup> I. Carusotto,<sup>1</sup> and N. Goldman<sup>3,\*</sup>

<sup>1</sup>INO-CNR BEC Center and Dipartimento di Fisica, Università di Trento, I-38123 Povo, Italy

<sup>2</sup>Institute for Theoretical Physics, ETH Zurich, 8093 Zürich, Switzerland

<sup>3</sup>CENOLI, Faculté des Sciences, Université Libre de Bruxelles (U.L.B.), B-1050 Brussels, Belgium  
(Received 21 May 2015; revised manuscript received 22 July 2015; published 3 November 2015)

We propose a realistic scheme to detect the 4D quantum Hall effect using ultracold atoms. Based on contemporary technology, motion along a synthetic fourth dimension can be accomplished through controlled transitions between internal states of atoms arranged in a 3D optical lattice. From a semiclassical analysis, we identify the linear and nonlinear quantized current responses of our 4D model, relating these to the topology of the Bloch bands. We then propose experimental protocols, based on current or center-of-mass-drift measurements, to extract the topological second Chern number. Our proposal sets the stage for the exploration of novel topological phases in higher dimensions.

DOI: 10.1103/PhysRevLett.115.195303

PACS numbers: 67.85.-d, 03.65.Sq, 37.10.Jk, 73.43.-f

In the past decade, there have been rapid developments in the control of coherent quantum systems. These advances have led to the experimental exploration of fundamental quantum mechanical concepts, many of which were previously only of theoretical interest. Specifically, fascinating artificial systems can now be engineered with atoms in optical lattices, where topological order, gauge structures, disorder, and interactions can all be tuned and probed in novel ways [1–3]. One such important recent achievement has been the realization of artificial magnetic fields and topological Bloch bands using time-modulated two-dimensional (2D) optical lattices [4–8].

Optical lattices can be tailored to realize lattice geometries of varying spatial dimensions  $d_{\text{real}} = 1, 2, 3$ . Moreover, increasing control over atomic internal states [1–3,9,10] has extended design flexibility as “motion” along an auxiliary (synthetic) dimension can be mimicked by laser-induced transitions between internal states [11–14]. This effectively generates dynamics within synthetic geometries with  $d = (d_{\text{real}} + 1)$  “spatial” dimensions, in addition to the usual time dimension. This was recently demonstrated in experiments, where 2D physics was explored with atoms in a one-dimensional optical lattice with a synthetic dimension [15,16]. These developments naturally open up the possibility of emulating systems with higher dimensions  $d > 3$ . For example, adding a synthetic dimension to a three-dimensional (3D) optical lattice would simulate a system in four dimensions (4D). Importantly, artificial gauge potentials [2,3] can naturally be introduced in atomic systems with synthetic dimensions [12] in the form of Peierls phase factors. These gauge structures can be finely tuned through the laser coupling, allowing experiments to explore topologically nontrivial energy bands in higher spatial dimensions.

In the fast-expanding field of topological phases of matter, the energy bands of a system are associated with

topological indices that are robust to continuous deformations. Nontrivial indices are usually associated with interesting boundary phenomena, quantized responses, and exotic quasiparticles [17,18]. In the 2D quantum Hall (QH) effect, the quantized Hall conductance is related to the sum of the first Chern numbers (1CNs) of the filled energy bands [19]. In 4D, even more intriguing quantum Hall phases may exist, as first predicted for time-reversal (TR) symmetric systems [20,21]. In the 4D QH effect, energy bands possess an additional nontrivial topological index, the second Chern number (2CN), leading to a nonlinear quantized response [20–22]. Both the 2D and 4D QH effects exhibit a variety of exotic strongly correlated phases in the presence of interactions [20,23]. Hence, 4D models with nonvanishing 2CNs have attracted much theoretical attention [21,24–28].

In this Letter, we describe a concrete proposal for realizing the 4D QH effect using ultracold gases in optical lattices. We present a semiclassical analysis predicting the general transport equations in 4D setups: this includes a nonlinear response, related to the 2CN, but also a linear response, associated with an exotic 2D QH effect for the current flowing across 2D planes within the 4D system. We then propose realistic protocols through which these responses could be measured experimentally.

*Semiclassical analysis.*—We consider particles of charge  $q = -1$  [29], moving in a lattice system and prepared in a nondegenerate energy band  $\mathcal{E}(\mathbf{k})$ . The geometrical properties of the Bloch band’s eigenstates  $|u\rangle$  are encoded in the Berry curvature 2-form [30],  $\Omega = (1/2)\Omega^{\mu\nu}(\mathbf{k})dk_\mu \wedge dk_\nu$ , with components  $\Omega^{\mu\nu} = i(\langle \partial_{k_\mu} u | \partial_{k_\nu} u \rangle - \langle \partial_{k_\nu} u | \partial_{k_\mu} u \rangle)$ . The indices  $\mu$  run over spatial coordinates with Einstein summation convention, and we set  $\hbar = 1$  unless otherwise stated. Specifically, we are interested in transport under external (weak) electric  $\mathbf{E} = E_\mu \mathbf{e}^\mu$  and magnetic fields, where  $B_{\mu\nu} = \partial_\mu A_\nu - \partial_\nu A_\mu$  is the magnetic field strength

and  $\mathbf{A} = A_\mu \mathbf{e}^\mu$  is the vector potential. We assume that any strong magnetic fields are directly incorporated into the Bloch band via the (magnetic) eigenstates  $|u\rangle$  [31]. Considering for now a system of arbitrary dimensions ( $d \geq 2$ ), we write the semiclassical equations of motion for a wave packet as [30–34]

$$\dot{\mathbf{r}}^\mu(\mathbf{k}) = \frac{\partial \mathcal{E}(\mathbf{k})}{\partial k_\mu} - \dot{k}_\nu \Omega^{\mu\nu}(\mathbf{k}), \quad (1)$$

$$\dot{k}_\mu = -E_\mu - \dot{r}^\nu B_{\nu\mu}, \quad (2)$$

where  $\mathbf{r} = r^\mu \mathbf{e}_\mu$  [resp.  $\mathbf{k} = k_\mu \mathbf{e}^\mu$ ] denotes the mean position [resp. quasimomentum] of the wave packet. We stress that the external fields  $E_\mu$  and  $B_{\mu\nu}$  are sufficiently weak perturbations that, at this level, the wave packet adiabatically follows the band  $\mathcal{E}(\mathbf{k})$  [35]. Next, we insert Eq. (2) into Eq. (1), in order to derive a transport equation relating the mean velocity to the external fields. To second order in the perturbations, this yields [35]

$$\begin{aligned} \dot{\mathbf{r}}^\mu(\mathbf{k}) &= \frac{\partial \mathcal{E}(\mathbf{k})}{\partial k_\mu} + E_\nu \Omega^{\mu\nu}(\mathbf{k}) + E_\delta B_{\nu\gamma} \Omega^{\gamma\delta}(\mathbf{k}) \Omega^{\mu\nu}(\mathbf{k}) \\ &+ \left( \frac{\partial \mathcal{E}(\mathbf{k})}{\partial k_\gamma} + \frac{\partial \mathcal{E}(\mathbf{k})}{\partial k_\alpha} \Omega^{\gamma\delta}(\mathbf{k}) B_{\delta\alpha} \right) \Omega^{\mu\nu}(\mathbf{k}) B_{\nu\gamma}. \end{aligned} \quad (3)$$

In addition to the group velocity of the band  $\partial_{k_\mu} \mathcal{E}$ , the first line of Eq. (3) includes two important response terms. The first of these corresponds to a transverse drift induced by the electric field, which is responsible for the QH effect in 2D; the second reveals a nonlinear (electromagnetic) response, which is quadratic in the Berry curvature. In this Letter, we are first interested in the transport of fermions completely filling the band  $\mathcal{E}(\mathbf{k})$ . In this case, neither the group velocity nor the terms in the second line of Eq. (3) contribute to the response [35]. Anticipating that the nonlinear term in the first line of Eq. (3) will be crucial when  $d \geq 4$ , as suggested by topological field theory [20,21], we now explicitly consider  $d = 4$ .

*4D transport equations and topological invariants.*—In the semiclassical approach, special care is required when evaluating the contribution of all the Bloch states in a given Bloch band [30]. An integration performed over phase space involves the usual density of states  $(1/2\pi)^d$  whenever either the external magnetic field or the Berry curvature is absent. However, in the presence of both quantities, the physical position and momentum must both be distinguished from the canonical coordinates, leading to a corresponding modification of the density of states [48–50]. In 4D, we find that the sum over all Bloch states can be accurately replaced by the integral [35]

$$\begin{aligned} \sum_{\mathbf{k}} &\equiv \frac{V}{(2\pi)^4} \int_{\mathbb{T}^4} \left[ 1 + \frac{1}{2} B_{\mu\nu} \Omega^{\mu\nu} \right. \\ &\left. + \frac{1}{64} (\varepsilon^{\alpha\beta\gamma\delta} B_{\alpha\beta} B_{\gamma\delta}) (\varepsilon_{\mu\nu\lambda\rho} \Omega^{\mu\nu} \Omega^{\lambda\rho}) \right] d^4 k, \end{aligned} \quad (4)$$

where indices now take values  $\mu = x, y, z, w$ ,  $V$  is the system's volume,  $\varepsilon^{\alpha\beta\gamma\delta}$  is the 4D Levi-Civita symbol, and where the integration is over the first (magnetic) Brillouin zone ( $\mathbb{T}^4$ ). One readily verifies that Eq. (4) generalizes the phase-space integration previously derived for 3D systems [48]. Combining Eq. (4) with Eq. (3) one obtains the transport for a filled band, i.e., defining the current density  $\mathbf{j}^\mu = \sum_{\mathbf{k}} \dot{\mathbf{r}}^\mu(\mathbf{k})/V$  yields [35]

$$\mathbf{j}^\mu = E_\nu \frac{1}{(2\pi)^4} \int_{\mathbb{T}^4} \Omega^{\mu\nu} d^4 k + \frac{\nu_2}{4\pi^2} \varepsilon^{\mu\alpha\beta\nu} E_\nu B_{\alpha\beta}, \quad (5)$$

introducing the 2CN [20,21,51,52,55]

$$\begin{aligned} \nu_2 &= \frac{1}{8\pi^2} \int_{\mathbb{T}^4} \Omega \wedge \Omega \in \mathbb{Z}, \\ &= \frac{1}{4\pi^2} \int_{\mathbb{T}^4} \Omega^{xy} \Omega^{zw} + \Omega^{wx} \Omega^{zy} + \Omega^{zx} \Omega^{yw} d^4 k. \end{aligned} \quad (6)$$

The transport equation, Eq. (5), is a central result of this work; it was derived from the semiclassical equations of motion [Eqs. (1) and (2)], without any assumptions about the system beyond the nondegeneracy of the Bloch band. The only two contributions for the filled band are a linear response, reminiscent of the 2D quantum Hall effect [19], and a nonlinear response proportional to the 2CN. We emphasise that the latter effect only takes place in systems of dimension  $d \geq 4$ , as formally imposed by the Levi-Civita symbol. This 4D QH effect was originally derived from a topological-field-theory approach [20,21] for TR-symmetric spinful systems, where the linear response vanishes by symmetry [56]. We note that 2CNs were previously studied from semiclassics in the polarization of inhomogenous crystals [57]. The transport equation, Eq. (5), can also be derived from a Streda-formula approach [35].

*Realistic physical system.*—We now describe our experimental proposal for observing 4D QH physics [Eq. (5)] based on cold-atom technology. As is clear from Eq. (6), a nontrivial 2CN requires that the Berry curvature has non-zero components in “disconnected” planes, e.g.,  $\Omega^{zx}$ ,  $\Omega^{yw} \neq 0$ . This sets a constraint on the minimal models displaying nontrivial 4D bands. Inspired by Ref. [28], we propose to build a 4D lattice in which the  $x$ - $z$  and  $y$ - $w$  planes are penetrated by uniform magnetic fluxes  $\Phi_{1,2}$ , respectively. This corresponds to two copies of the Hofstadter model [58] defined in disconnected planes. The Hamiltonian is thus of the tight-binding form

$$\hat{H} = -J \sum_{\mathbf{r}} c_{\mathbf{r}+ae_x}^\dagger c_{\mathbf{r}} + c_{\mathbf{r}+ae_y}^\dagger c_{\mathbf{r}} + e^{i2\pi\Phi_1 x/a} c_{\mathbf{r}+ae_z}^\dagger c_{\mathbf{r}} + e^{i2\pi\Phi_2 y/a} c_{\mathbf{r}+ae_w}^\dagger c_{\mathbf{r}} + \text{H.c.}, \quad (7)$$

where  $c_{\mathbf{r}}^\dagger$  creates a fermion at lattice site  $\mathbf{r} = (x, y, z, w)$ ,  $a$  is the lattice spacing,  $J$  is the hopping amplitude [Fig. 1(a)]. This model has two main ingredients: (i)  $x$ -dependent Peierls phase factors for tunneling along the  $z$  direction, generating a uniform flux  $\Phi_1$  in the  $x$ - $z$  plane, and (ii)  $y$ -dependent Peierls phase factors for tunneling along the  $w$  direction, creating a uniform flux  $\Phi_2$  in the  $y$ - $w$  plane. The first ingredient, (i), can be engineered using the method implemented in Refs. [5–7], i.e., by combining a superlattice (or a Wannier-Stark ladder) along the  $z$  direction with a resonant time modulation of the optical-lattice potential [59–61]. The second ingredient, (ii), requires an extra (synthetic) dimension [11,12,15,16], which can be simulated by adjusting two-photon Raman coupling to induce transitions between different internal atomic states [35]. The Raman wave vector should be aligned along the  $y$  direction so as to realize  $y$ -dependent Peierls phase factors [Fig. 1(a)], as was successfully implemented in Refs. [15,16]. In general, hopping processes along the synthetic dimension are inhomogeneous [12,35], but we verified that this does not significantly alter the topological band properties studied below [35]. Hence, for the sake of simplicity, we assume the 4D system [Eq. (7)] is isotropic with a single hopping rate  $J$  for all hopping processes.

The bulk energy spectrum  $\mathcal{E}(\mathbf{k})$  of the model [Eq. (7)] is reminiscent of the two underlying (2D) Hofstadter models defined in the  $x$ - $z$  and  $y$ - $w$  planes [28,35]. Specifically, the

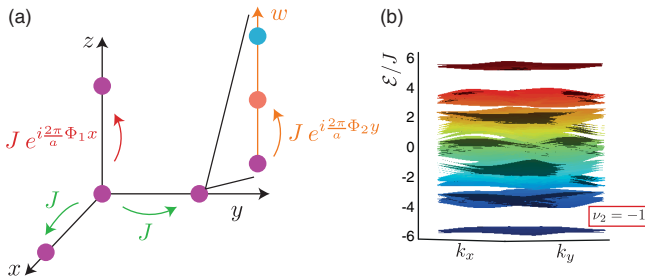


FIG. 1 (color online). (a) The 4D lattice in the absence of perturbing fields ( $E_\mu, B_{\mu\nu} = 0$ ). Atoms move in a 3D optical lattice, with hopping amplitude  $J$ . A Hofstadter model [58] is realized in the  $x$ - $z$  plane, with flux  $2\pi\Phi_1$  per unit cell, from  $x$ -dependent Peierls phase factors in the hopping along the  $z$  direction [5–7]. A fourth (synthetic) dimension [11,12], with coordinate  $w$ , is accessible at each lattice site, as Raman coupling induces internal-state transitions [35]. A second Hofstadter model, with flux  $2\pi\Phi_2$ , is realized in the  $y$ - $w$  plane by adding a  $y$ -dependent phase factor to the internal-state transitions, i.e., by aligning the Raman wave vector along the  $y$  direction [12,15,16]. (b) Energy spectrum  $\mathcal{E}(k_x, k_y)$  for  $\Phi_{1,2} = 1/4$ , and for many values  $k_{z,w}$  over the Brillouin zone; the 2CN of the lowest (nondegenerate) band is indicated.

spectrum corresponds to the Minkowski sum  $\mathcal{E} = \{E_1 + E_2 | E_1 \in \mathcal{E}_{xz}, E_2 \in \mathcal{E}_{yw}\}$ , where  $\mathcal{E}_{xz}$  and  $\mathcal{E}_{yw}$  denote the spectra associated with the 2D Hofstadter models [35]. This rich 4D spectrum has a lowest band  $\mathcal{E}_1(\mathbf{k})$ , which is generally nondegenerate and, for suitable fluxes of the form  $\Phi_1 = 1/q_1$  and  $\Phi_2 = 1/q_2$  with  $q_1, q_2 \in \mathbb{Z}$ , can be well isolated from higher-energy bands. This happens, for example, for fluxes  $\Phi_{1,2} = 1/4$  where the lowest band  $\mathcal{E}_1(\mathbf{k})$  has a large flatness ratio  $\Delta/W \approx 3$ , for bandwidth  $W$  and the lowest bulk gap  $\Delta \approx 1.3J$  [Fig. 1(b)]. We henceforth focus on this choice of  $\Phi_{1,2}$ , as it is relevant to recent experiments on the 2D Hofstadter model [5,7].

The bulk spectrum also inherits the topological properties of the underlying Hofstadter models [28,35]. The lowest band  $\mathcal{E}_1(\mathbf{k})$  is characterized by a nonzero 2CN [62], which can be factorized as  $\nu_2 = \nu_1^{zx} \times \nu_1^{yw}$ , where we introduced the 1CNs associated with the lowest bands of the 2D spectra  $\mathcal{E}_{xz}$  and  $\mathcal{E}_{yw}$ , respectively [35]. Note that the 4D Berry curvature  $\Omega^{\mu\nu}$  and the 2CN  $\nu_2$  of the lowest band can be evaluated numerically, with a 4D generalization [35] of the method developed in Ref. [63].

*Response of the system to external fields.*—We now investigate the transport equations [Eq. (5)] with external “electric”  $E_\mu$  and “magnetic”  $B_{\mu\nu}$  fields. As the atoms are neutral, the electric field  $E_\mu$  corresponds here to a linear gradient, which can either be magnetically [5,6] or optically [7] created. The perturbing magnetic field  $B_{\mu\nu}$  can be generated by engineering additional Peierls phase factors. For the sake of experimental simplicity, we choose the weak field  $B_{\mu\nu}$  to have a single nonzero component,  $B_{zw} = -2\pi\tilde{\Phi}/a^2$ , as is readily achieved by adding an extra  $z$ -dependent phase factor to internal-state transitions [64]; this occurs in our proposed system if the Raman wave vector is tilted in the  $y$ - $z$  plane. To isolate the linear and nonlinear responses, we align the electric field along the  $y$  direction,  $\mathbf{E} = E_y \mathbf{e}^y$ . The transport equations [Eq. (5)] are then explicitly  $j^y = j^z = 0$ , and

$$j^x = \frac{\nu_2}{4\pi^2} E_y B_{zw} = -\frac{\nu_2}{2\pi a^2} E_y \tilde{\Phi}, \quad (8)$$

$$j^w = E_y \frac{1}{(2\pi)^4} \int_{\mathbb{T}^4} \Omega^{wy} d^4 k = -\frac{\nu_1^{yw}}{2\pi a^2 q_1} E_y. \quad (9)$$

Importantly, Eq. (8) reveals a genuine nonlinear 4D-QH response along the  $x$  direction. In Eq. (9), we have highlighted the 1CN  $\nu_1^{yw}$  associated with the  $y$ - $w$  plane [65], and have used that the flux is  $\Phi_1 = 1/q_1$  in the  $x$ - $z$  plane. Hence, Eq. (9) shows that an exotic 2D QH effect takes place in the  $y$ - $w$  plane: defining the Hall conductivity in this plane as  $\sigma_{wy} = j_{\text{2D}}^w / E_y = a^2 j^w / E_y$ , we find

$$\sigma_{wy} = -(e^2/h) \nu_1^{yw} / q_1, \quad q_1, \nu_1^{yw} \in \mathbb{Z}, \quad (10)$$

where the conductivity quantum  $e^2/h$  is reintroduced. Such a “fractional QH effect” is allowed in noninteracting

systems provided the associated 2D plane is embedded in a higher-dimensional system [18], as recently shown in 3D topological insulators [66]. Here, the fractionalization of the Hall conductivity  $\sigma_{wy}$  reflects the change in size of the magnetic Brillouin zone due to the flux  $\Phi_1 = 1/q_1$  penetrating the disconnected plane  $x$ - $z$ .

*Numerical calculations.*—In order to test the predictions in Eqs. (8) and (9), we have numerically calculated the current density  $j^\mu$  in a 4D lattice system filling the lowest bulk band. The plots in Fig. 2(a) show the quasistationary current density  $j^\mu$  obtained after ramping up the field  $E_y$  to the final value  $E_y = -0.2J/a$ , which was chosen so as to limit interband transitions [7,67,68]. Comparing these numerical results to Eqs. (8) and (9) allows one to extract the topological indices: we find  $\nu_2 \approx -1.07$  and  $\nu_1^{yw} \approx -1.03$ , in agreement with the topological band structure ( $\nu_2 = \nu_1^{yw} = -1$ ). These simulations also validate

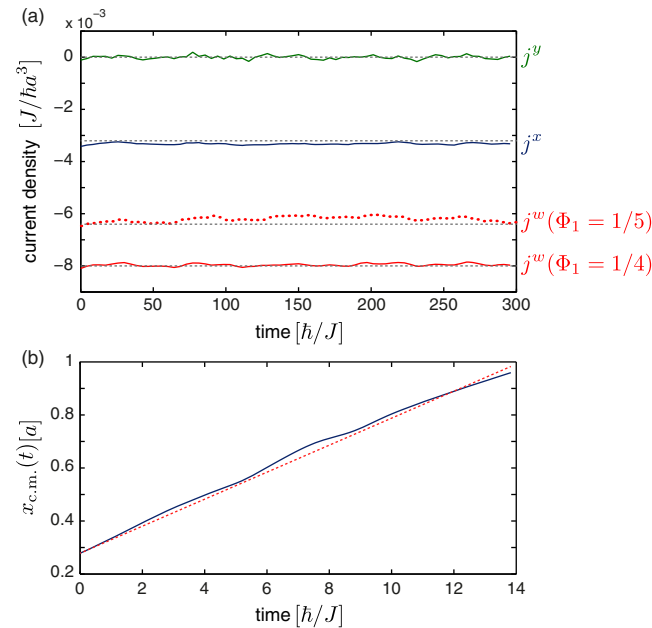


FIG. 2 (color online). (a) Current density  $j^\mu(t)$  after ramping up the electric field to  $E_y = -0.2J/a$ . The fluxes were taken  $\Phi_{1,2} = 1/4$ , and the Fermi energy  $E_F = -5J$  was set in the first bulk energy gap [see Fig. 1(b)]. The perturbing magnetic field was chosen as  $B_{zw} = -2\pi\tilde{\Phi}/a^2 = -\pi/5a^2$ . Simulations were performed on a  $8 \times 10 \times 10 \times 4$  lattice, with periodic boundary conditions along the  $x$ ,  $z$ ,  $w$  directions. The component  $j^w$  was also calculated for  $\Phi_1 = 1/5$  (red dotted line). Black lines show predictions [Eqs. (8) and (9)] for  $\nu_2 = \nu_1^{yw} = -1$ . (b) Center-of-mass trajectory  $x_{c.m.}(t)$  after ramping up the electric field to  $E_y = 0.2J/a$ ; the nonlinear response is in the opposite direction to (a) as  $E_y$  is reversed. Simulations are for a  $12 \times 12 \times 10 \times 4$  lattice, with periodic boundary conditions along the  $z$ ,  $w$  directions. The initial radius of the cloud was  $r_0 = 4a$  in the  $x$ - $y$  plane. The fluxes are  $\Phi_{1,2} = 1/4$ , with all other parameters the same as in (a). The red dotted curve shows the predicted drift,  $v_{c.m.}^x = j^x \times 16a^4 = -8a^2\nu_2 E_y \tilde{\Phi}/\pi$ , for  $\nu_2 = -1$ .

the  $\Phi_1$  dependence in Eqs. (9) and (10), as we see that  $j^w$  is indeed reduced by a factor  $4/5$  when changing the flux  $\Phi_1 = 1/4 \rightarrow 1/5$  in the  $x$ - $z$  plane.

While current measurements could be performed in cold-atom experiments [69,70], e.g., by generalizing the method of Ref. [71], a more accessible probe of the topological transport would be the observation of the center-of-mass (c.m.) motion of the cloud [7,68]. The c.m. velocity for this system is  $v_{c.m.}^\mu = j^\mu V_{\text{cell}}$ , where  $j^\mu$  is given in Eqs. (8) and (9), and  $V_{\text{cell}}$  is the (magnetic) unit cell volume [7,68,72], which is  $V_{\text{cell}} = 16a^4$  for  $\Phi_{1,2} = 1/4$ . For a perturbing flux  $\tilde{\Phi} = 1/10$ , we find that the 2CN response should lead to a drift along the  $x$  direction with  $v_{c.m.}^x \approx 2a/T_B$ , where  $T_B = 2\pi/aE_y \approx 50$  ms is a typical Bloch oscillation time [7]. Such a cloud displacement is of the same order as the one reported in the recent 1CN measurement [7]. We analyzed the c.m. displacement  $x_{c.m.}(t)$  by simulating a 4D system with open boundary conditions in the  $x$ ,  $y$  directions. Numerically, the cloud is initially confined in the presence of all fluxes, then the confinement is removed and the electric field is ramped up [68]. From the c.m. drift in Fig. 2(b), we extract a realistic “experimental” value for the 2CN:  $\nu_2 \approx -0.98$ .

*Discussion.*—The c.m. response, presented in Fig. 2(b) for a Fermi system initially filling the lowest energy band, is strictly identical to that obtained if the band is uniformly, but only partially, filled [35]. This situation typically occurs when a thermal gas is loaded into an energy band with a large flatness ratio [7], such as the lowest band in Fig. 1(b). Consequently, the 4D QH physics discussed here could equally be explored using Fermi or Bose gases [7]. We note that other external-field configurations could be chosen to fully test the 4D physics in Eq. (5). We also stress that an accurate measurement of the 2CN requires a large number of internal states [35]; this can be solved experimentally by imposing periodic boundary conditions along the synthetic dimension, as could be realized with an extra Raman coupling [12]. Finally, we note that the topological gap  $\Delta \approx 1.3J$  is of the same order as in Ref. [7]; this requires low but achievable temperatures to extract the band’s topology (see Ref. [7] for methods to extract the Chern number in the presence of band repopulation, and Ref. [73] on heating sources).

*Conclusion.*—We have proposed a realistic physical platform to observe the 4D QH effect in cold-atom transport experiments [7,8,67,68]. We have highlighted the minimal requirements for measuring a nontrivial 2CN in an atomic system, exploiting Raman transitions between internal states [12]. Our proposal sets the stage for the future experimental exploration of higher-dimensional topological phases. The principles of our setup could also be extended beyond cold atoms, for example, to photonic systems [74]. Realizing such 4D systems experimentally will be especially intriguing as they may harbor exotic collective excitations [20].

We thank N. R. Cooper, J. Dalibard, A. Celi, I. Bloch, M. Aidelsburger, C. Weitenberg, L. Fallani, P. Massignan, M. Lewenstein, A. Dauphin, P. Gaspard, J. Catani, C. Sias, L. Mazza, K. Kraus, and Z. Ringel for fruitful discussions. H. M. P., T. O. and I. C. were funded by ERC through the QGBE grant, by the EU-FET Proactive grant AQUUS (Project No. 640800), and by Provincia Autonoma di Trento, partially through the project “On silicon chip quantum optics for quantum computing and secure communications—SiQuro”. O.Z. acknowledges the Swiss National Foundation for financial support. N. G. is financed by the FRS-FNRS Belgium and by the BSPO under the PAI project P7/18 DYGEST.

\*ngoldman@ulb.ac.be

- [1] I. Bloch, J. Dalibard, and W. Zwerger, *Rev. Mod. Phys.* **80**, 885 (2008).
- [2] J. Dalibard, F. Gerbier, G. Juzeliūnas, and P. Öhberg, *Rev. Mod. Phys.* **83**, 1523 (2011).
- [3] N. Goldman, G. Juzeliūnas, P. Öhberg, and I. B. Spielman, *Rep. Prog. Phys.* **77**, 126401 (2014).
- [4] J. Struck, M. Weinberg, C. Ölschläger, P. Windpassinger, J. Simonet, K. Sengstock, R. Höppner, P. Hauke, A. Eckardt, M. Lewenstein, and L. Mathey, *Nat. Phys.* **9**, 738 (2013).
- [5] M. Aidelsburger, M. Atala, M. Lohse, J. T. Barreiro, B. Paredes, and I. Bloch, *Phys. Rev. Lett.* **111**, 185301 (2013).
- [6] H. Miyake, G. A. Siviloglou, C. J. Kennedy, W. C. Burton, and W. Ketterle, *Phys. Rev. Lett.* **111**, 185302 (2013).
- [7] M. Aidelsburger, M. Lohse, C. Schweizer, M. Atala, J. T. Barreiro, S. Nascimbène, N. R. Cooper, I. Bloch, and N. Goldman, *Nat. Phys.* **11**, 162 (2015).
- [8] G. Jotzu, M. Messer, R. Desbuquois, M. Lebrat, T. Uehlinger, D. Greif, and T. Esslinger, *Nature (London)* **515**, 237 (2014).
- [9] D. Jaksch and P. Zoller, *Ann. Phys. (Amsterdam)* **315**, 52 (2005).
- [10] C. Weitenberg, M. Endres, J. F. Sherson, M. Cheneau, P. Schauß, T. Fukuhara, I. Bloch, and S. Kuhr, *Nature (London)* **471**, 319 (2011).
- [11] O. Boada, A. Celi, J. I. Latorre, and M. Lewenstein, *Phys. Rev. Lett.* **108**, 133001 (2012).
- [12] A. Celi, P. Massignan, J. Ruseckas, N. Goldman, I. B. Spielman, G. Juzeliūnas, and M. Lewenstein, *Phys. Rev. Lett.* **112**, 043001 (2014).
- [13] N. R. Cooper and A. M. Rey, *Phys. Rev. A* **92**, 021401(R) (2015).
- [14] S. Barbarino, L. Taddia, D. Rossini, L. Mazza, and R. Fazio, *Nat. Commun.* **6**, 8134 (2015).
- [15] M. Mancini, G. Pagano, G. Cappellini, L. Livi, M. Rider, J. Catani, C. Sias, P. Zoller, M. Inguscio, M. Dalmonte, and L. Fallani, *Science* **349**, 1510 (2015).
- [16] B. K. Stuhl, H. I. Lu, L. M. Ayccock, D. Genkina, and I. B. Spielman, *Science* **349**, 1514 (2015).
- [17] M. Z. Hasan and C. L. Kane, *Rev. Mod. Phys.* **82**, 3045 (2010).
- [18] X.-L. Qi and S.-C. Zhang, *Rev. Mod. Phys.* **83**, 1057 (2011).
- [19] D. J. Thouless, M. Kohmoto, M. P. Nightingale, and M. den Nijs, *Phys. Rev. Lett.* **49**, 405 (1982).
- [20] S.-C. Zhang and J. Hu, *Science* **294**, 823 (2001).
- [21] X.-L. Qi, T. L. Hughes, and S.-C. Zhang, *Phys. Rev. B* **78**, 195424 (2008).
- [22] C. Yang, *J. Math. Phys. (N.Y.)* **19**, 320 (1978).
- [23] C. Nayak, S. H. Simon, A. Stern, M. Freedman, and S. Das Sarma, *Rev. Mod. Phys.* **80**, 1083 (2008).
- [24] Y. Li, S.-C. Zhang, and C. Wu, *Phys. Rev. Lett.* **111**, 186803 (2013).
- [25] Y. Li, K. Intriligator, Y. Yu, and C. Wu, *Phys. Rev. B* **85**, 085132 (2012).
- [26] Y. Li and C. Wu, *Phys. Rev. Lett.* **110**, 216802 (2013).
- [27] J. M. Edge, J. Tworzydło, and C. W. J. Beenakker, *Phys. Rev. Lett.* **109**, 135701 (2012).
- [28] Y. E. Kraus, Z. Ringel, and O. Zeitler, *Phys. Rev. Lett.* **111**, 226401 (2013).
- [29] The discussion is general and also applies to neutral particles, in which case the external fields are artificial [2,3].
- [30] D. Xiao, M.-C. Chang, and Q. Niu, *Rev. Mod. Phys.* **82**, 1959 (2010).
- [31] M.-C. Chang and Q. Niu, *Phys. Rev. B* **53**, 7010 (1996).
- [32] This should also contain corrections to the band energy and Berry curvature from the external fields [33]. However, as these play no role in the 4D transport of a filled band, the full semiclassical analysis (to second-order in the fields) is left to the Supplemental Material.
- [33] Y. Gao, S. A. Yang, and Q. Niu, *Phys. Rev. Lett.* **112**, 166601 (2014).
- [34] M.-C. Chang and Q. Niu, *Phys. Rev. Lett.* **75**, 1348 (1995).
- [35] See Supplemental Material at <http://link.aps.org/supplemental/10.1103/PhysRevLett.115.195303>, which includes Refs. [36–47], for a full discussion of the semiclassical analysis, including the modified density of states; of the Streda-Widom approach; of the spectral and topological properties of our proposed model; of a numerical method evaluating the second Chern number; of the effects of partial band-filling; of boundary conditions and internal states requirements; and of the effects of anisotropy along the synthetic dimension.
- [36] Y. Gao, S. A. Yang, and Q. Niu, *Phys. Rev. B* **91**, 214405 (2015).
- [37] P. Gosselin, F. Ménas, A. Bérard, and H. Mohrbach, *Europhys. Lett.* **76**, 651 (2006).
- [38] D. Xiao, J. Shi, and Q. Niu, *Phys. Rev. Lett.* **96**, 099702 (2006).
- [39] L. D. Landau and L. M. Lifshitz, *Quantum Mechanics* 3rd ed. (Butterworth Heinemann, Oxford, 1958), Vol. 3.
- [40] E. N. Adams and E. I. Blount, *J. Phys. Chem. Solids* **10**, 286 (1959).
- [41] N. Nagaosa, J. Sinova, S. Onoda, A. H. MacDonald, and N. P. Ong, *Rev. Mod. Phys.* **82**, 1539 (2010).
- [42] K. Y. Bliokh and Y. P. Bliokh, *Ann. Phys. (Amsterdam)* **319**, 13 (2005).
- [43] P. Gosselin, A. Bérard, and H. Mohrbach, *Eur. Phys. J. B* **58**, 137 (2007).
- [44] A. Widom, *Phys. Lett. A* **90**, 474 (1982).
- [45] P. Streda, *J. Phys. C* **15**, L717 (1982).
- [46] P. Streda and L. Smrcka, *J. Phys. C* **16**, L895 (1983).
- [47] D. L. Bergman and G. Refael, *Phys. Rev. B* **87**, 024202 (2013).
- [48] D. Xiao, J. Shi, and Q. Niu, *Phys. Rev. Lett.* **95**, 137204 (2005).

- [49] C. Duval, Z. Horváth, P. A. Horváthy, L. Martina, and P. C. Stichel, *Mod. Phys. Lett. B* **20**, 373 (2006).
- [50] K. Yu. Bliokh, *Phys. Lett. A* **351**, 123 (2006).
- [51] J. E. Avron, L. Sadun, J. Segert, and B. Simon, *Phys. Rev. Lett.* **61**, 1329 (1988).
- [52] This is the 2CN defined from the Chern character rather than the Chern class [53,54].
- [53] M. Nakahara, *Geometry, Topology and Physics* (IOP Publishing Ltd., Bristol and Philadelphia, 2003).
- [54] S. Ryu, A. P. Schnyder, A. Furusaki, and A. W. W. Ludwig, *New J. Phys.* **12**, 065010 (2010).
- [55] T. Fukui, T. Fujiwara, and Y. Hatsugai, *J. Phys. Soc. Jpn.*, **77**, 123705 (2008).
- [56] In this case, the Bloch bands can contain Kramers degeneracies [17,18].
- [57] D. Xiao, J. Shi, D. P. Clougherty, and Q. Niu, *Phys. Rev. Lett.* **102**, 087602 (2009).
- [58] D. R. Hofstadter, *Phys. Rev. B* **14**, 2239 (1976).
- [59] A. R. Kolovsky, *Europhys. Lett.* **93**, 20003 (2011).
- [60] A. Bermudez, T. Schaetz, and D. Porras, *Phys. Rev. Lett.* **107**, 150501 (2011).
- [61] N. Goldman, J. Dalibard, M. Aidelsburger, and N. R. Cooper, *Phys. Rev. A* **91**, 033632 (2015).
- [62] In contrast to the TR-symmetric models of Refs. [20,21], the present (spinless) model [Eq. (7)] explicitly breaks TR symmetry, and formally has a trivial Chern class but a nontrivial Chern character [53,54]; see Ref. [28] where a spin-1/2 version of Eq. (7) was introduced.
- [63] T. Fukui, Y. Hatsugai, and H. Suzuki, *J. Phys. Soc. Jpn.* **74**, 1674 (2005).
- [64] Following our convention for the Peierls phase factors [see Fig. 1(a)], the magnetic field strength felt by a particle of charge  $q = -1$  is  $B_{\mu\nu} = -2\pi\Phi_{\mu\nu}/a^2$ ; in the text, the strong fluxes are  $\Phi_1 = \Phi_{xz}$ ,  $\Phi_2 = \Phi_{yw}$  and the perturbing flux is  $\tilde{\Phi} = \Phi_{zw}$ .
- [65] Note that  $\nu_1^{yw} = (1/2\pi)\int\Omega^{yw}dk_ydk_w = -(1/2\pi)\int\Omega^{wy}dk_ydk_w$  where the integral is over the  $k_y$ - $k_w$  Brillouin zone [35].
- [66] Y. Xu, I. Miotkowski, C. Liu, J. Tian, H. Nam, N. Alidoust, J. Hu, C.-K. Shih, M. Z. Hasan, and Y. P. Chen, *Nat. Phys.* **10**, 956 (2014).
- [67] H. M. Price and N. R. Cooper, *Phys. Rev. A* **85**, 033620 (2012).
- [68] A. Dauphin and N. Goldman, *Phys. Rev. Lett.* **111**, 135302 (2013).
- [69] I. Bloch (private communication).
- [70] J.-P. Brantut, J. Meineke, D. Stadler, S. Krinner, and T. Esslinger, *Science* **337**, 1069(2012).
- [71] M. Atala, M. Aidelsburger, M. Lohse, J. T. Barreiro, B. Paredes, and I. Bloch, *Nat. Phys.* **10**, 588 (2014).
- [72] The current density is  $\mathbf{j} = \mathbf{v}_{\text{tot}}/V$ , while the c.m. velocity is  $\mathbf{v}_{\text{c.m.}} = \mathbf{v}_{\text{tot}}/N_{\text{tot}}$ , where  $N_{\text{tot}}$  is the particle number and  $\mathbf{v}_{\text{tot}}$  is the total velocity. Combining these,  $\mathbf{v}_{\text{c.m.}} = \mathbf{j}/n$  with  $n$  being the particle density of the filled band. For this case,  $n = 1/V_{\text{cell}}$ , and so  $\mathbf{v}_{\text{c.m.}} = \mathbf{j}V_{\text{cell}}$ .
- [73] T. Bilitewski and N. R. Cooper, *Phys. Rev. A* **91**, 033601 (2015); **91**, 063611 (2015); S. Choudhury and E. J. Mueller, *Phys. Rev. A* **91**, 023624 (2015).
- [74] T. Ozawa, H. M. Price, N. Goldman, O. Zilberberg, I. Carusotto, [arXiv:1510.03910](https://arxiv.org/abs/1510.03910).